

ICSGCE 2011: 27–30 September 2011, Chengdu, China

Measurement of Wind Speed and Direction with Ultrasonic Sensor Using FPGA

Kuojun Xie^{*}, Kuijun Wang

School of Physical Electronics, University of Electronic Science and Technology of China, Chengdu, 610054, China

Abstract

In this paper we introduce the method of measurement of wind speed and direction based on an embedded system with multiple ultrasonic sensor. The system includes front-end circuits and back-end circuits. The Front-end circuits include the sensor's low-voltage drive circuit, preamplifier circuit, filter circuit, the voltage comparator circuit and the signal isolation circuit. Back-end circuits include the signal generator circuit, the signal detection circuit, FIFO circuit, LCD driver circuit and UART protocol Circuit. Using low voltage drive drives the sensor can reduce the debugging of the system. The system can launch and receive ultrasonic signal, and get the time of flight of ultrasonic signal according to design precision after verification. All control and processing are in Field Programmable Gate Array (FPGA). FPGA is the very key factor in system design.

© 2011 Published by Elsevier Ltd. Selection and/or peer-review under responsibility of University of Electronic Science and Technology of China (UESTC).

Keywords: Ultrasonic sensor; Wind speed and direction; Time difference; Low voltage drive; FPGA

1. Introduction

With the rapid development of global economy, the increasing demand of energy is widely concerned. Wind power is a kind of clean, renewable energy. Since 80s and 90s of last century, it has experienced rapid development. In the new energy field, it is the power generation method which has the most mature technology, as well as extending scale of commercial development prospects[1][2]. However, wind power costs more than other powers; and an important factor is the stability problem of wind power[3][4][5]. Because win speed is random, on the wind site, we should measure the speed and direction accurately and timely in order to control the fan well. Compared with the traditional indicators, ultrasonic wind speed and direction indicator has many advantages such as high accuracy, no abrasion. In China, the research on ultrasonic instrumentation started relatively late. The cheaper instruments are also

^{*} Corresponding author. Tel.: +86-15982818780.

E-mail address: xkj@uestc.edu.cn.

rare in market [6].

2. Principle of Operation

By using ultrasonic, several methods can be used to measure the fluid, such as time difference method, Doppler method, vortex method and correlation method, etc. These methods have advantages and disadvantages, and will be selected according to the accuracy and environment in practical application. In this design, we use the time difference method.

There are four ultrasonic sensors in the system. Those are installed in four directions as shown in Fig. 1.

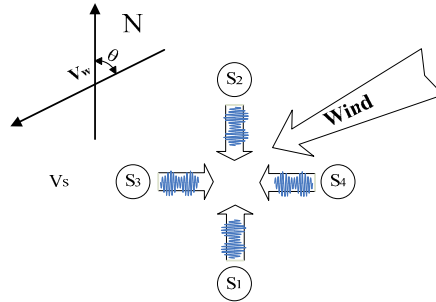


Fig. 1. Time difference measurement configuration

The time of flight in this case can be given by,

$$t_{12} = \frac{L_{12}}{V_s - V_w \cos \theta} \quad (1)$$

$$t_{21} = \frac{L_{12}}{V_s + V_w \cos \theta} \quad (2)$$

$$t_{21} - t_{12} = \frac{2L_{12}V_w \cos \theta}{V_s^2 + V_w^2 \cos^2 \theta} \quad (3)$$

$$t_{21}t_{12} = \frac{2L_{12}V_w \cos \theta}{V_s^2 - V_w^2 \cos^2 \theta} \quad (4)$$

where,

L_{12} =Distance between sensor 1 and sensor 2 (m).

V_s = Propagation velocity of ultrasonic wave in the air (m/s).

t_{12} = Propagation time of ultrasonic signal from sensor 1 to sensor 2 (s).

t_{21} = Propagation time of ultrasonic signal from sensor 2 to sensor 1 (s).

V_w =The real-time wind speed (m/s).

Then (2) and (3) subtracted,

$$V_w \cos \theta = \frac{L_{12}(t_{21} - t_{12})}{t_{21}t_{12}} \quad (5)$$

$$V_w \sin \theta = \frac{L_{34}(t_{34} - t_{43})}{t_{34}t_{43}} \quad (6)$$

where:

$L_{23} = L_{12}$, distance between sensor 1 and sensor 2 (m)

t_{34} = Propagation time of ultrasonic signal from sensor 3 to sensor 4 (s)

t_{43} = Propagation time of ultrasonic signal from sensor 4 to sensor 3 (s)

(5) and (6), the wind direction can be determined as,

$$\tan \theta = \frac{t_{12}t_{21}(t_{34} - t_{43})}{t_{34}t_{43}(t_{21} - t_{12})} \quad (7)$$

$$\theta = \tan^{-1} \left[\frac{t_{12}t_{21}(t_{34} - t_{43})}{t_{34}t_{43}(t_{21} - t_{12})} \right] \quad (8)$$

3. System Design

The system design includes sensors, drive circuit, signal processing circuit, FPGA etc. as is shown in Figure 2. With the development of microelectronics technology, FPGA applications are increasingly widespread with more low cost and high performance advantages. In the hardware design, the final design chooses FPGA to reduce system development costs.

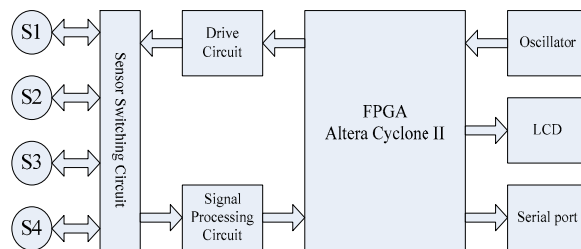


Fig. 2. Circuit diagram

3.1. Drive circuits

In this system, ultrasonic sensor drive circuit is an important part, and the center frequency of ultrasonic sensor is 200 kHz [7]. In traditional design, the drive circuit consists of transformer and power FET, which can provide enough energy. However it is very inconvenient for debugging, and it affects the system stability. To drive the sensor, the square wave can be generated by FPGA device through optical coupling circuit to control N channel FET. And transient high voltage pulse drive circuit can be generated by using the characteristics of inductor and capacitance.

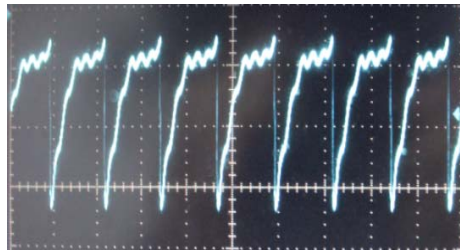


Fig. 3. Voltage of sensor

3.2. Signal processing circuits

The signal processing circuit includes pre-amplifier module, band-pass filter module, and voltage comparators module. As high frequency the ultrasonic signal attenuate [8], receiving sensor can receive the primary signal which is very weak.

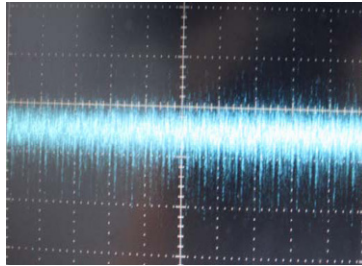


Fig. 4. Primary ultrasonic signal

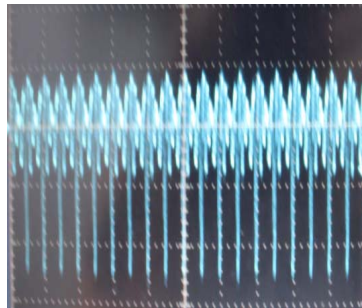


Fig. 5. Amplified ultrasonic signal

Fig. 5 shows the signal after the amplification, due to the noise around with the real ultrasonic signal amplification, signal processing for subsequent inconvenience to its filtering processing. In traditional circuit design, the filters are designed by inductor, resistance and capacitance, which have a simple structure. The design and debugging are inconvenient due to a large number of discrete components. In the filter module, we use the universal filter chip, Maxim's chip-max275. The max275 are continuous-time active filters which consist of independent cascadable 2nd-order sections. Each section can implement and all-pole bandpass or lowpass filter response, and it is programmed by four external resistors. The bandpass filter is shown in Fig. 6.

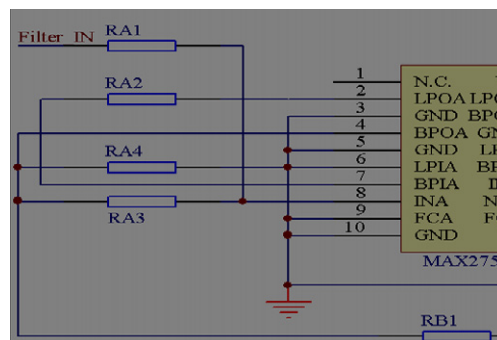


Fig. 6. Filter circuit

According to the datasheet [9], we can get the value of resistance from those equations:

$$F_0 = 200 \quad (8)$$

$$RA_2=RB_2 = \frac{(2 \times 10^9)}{F_0} \quad (9)$$

$$RA_4=RB_4 = RA_2 - 5 \quad (10)$$

$$RA_3=RB_3 = \frac{Q(2 \times 10^9)}{F_0} \times \left(\frac{RX}{RY} \right) \quad (11)$$

$$RA_1=RB_1 = \frac{2 \times 10^9}{F_0 H_{OBP}} \times \left(\frac{RX}{RY} \right) \quad (12)$$

where

F_0 =Sensor center frequency (kHz)

Q =Quality factor

H_{OBP} =Bandpass filter gain at F_0 (dB)

RX/R_Y =Connect FC to positive voltage, ground, and negative voltage, the value of RX/R_Y is 4, 1/5, and 1/25 respectively.

In the module, when we select the $Q=12$, we can get $RA_1=RB_1=24 \text{ k}\Omega$, $RA_2=RB_2=10 \text{ k}\Omega$, $RA_3=RB_3=24 \text{ k}\Omega$, $RA_4=RB_4=5 \text{ k}\Omega$ respectively. The output from the filter module is as shown in Fig. 7.

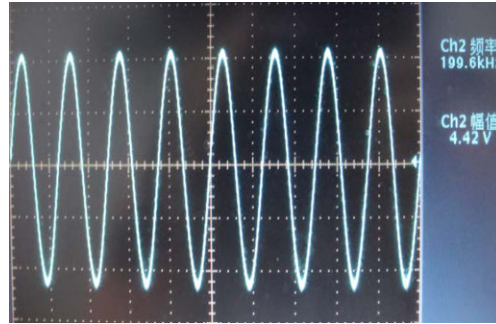


Fig. 7. Ultrasonic wave signal after filtering

4. FPGA Design

In the time difference method, the timing design is the core of the system, it tests the accuracy of the precision of a direct impact on speed. The device supports the operating frequency, 200 MHz that is 5 ns. FPGA block diagram consists of Finite State Machine (FSM), Signal Generator (SG), High-Speed Counter (HSC), Data Cache (DC) and so on.

In the system, we use the phase-locked loop (PLL) to frequency multiplication [10][11]. In FPGA circuit, in order to generate the signal, FSM module is used to control the SG module, then, the HSC module and SD module are working and processing. When the SD module detects the rising edge, FSM controls the SG module to stop to generate the signal, and close the HSC module. The data of HSC module will be sent to DC module. As is shown in Figure 9, $T_{compare}$ is a flag, T_1 is counter period, T_2 is the signal period, T_{tof1} and T_{tof2} are different time of flight because of the flag $T_{compare}$. If $T_{compare}$ is within allowable range, the data will be delivered through the Serial port. At the same time, the FSM starts to next counter using HDL[12].

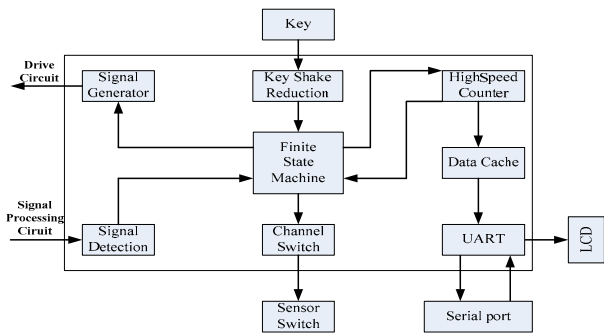


Fig. 8. FPGA block diagram

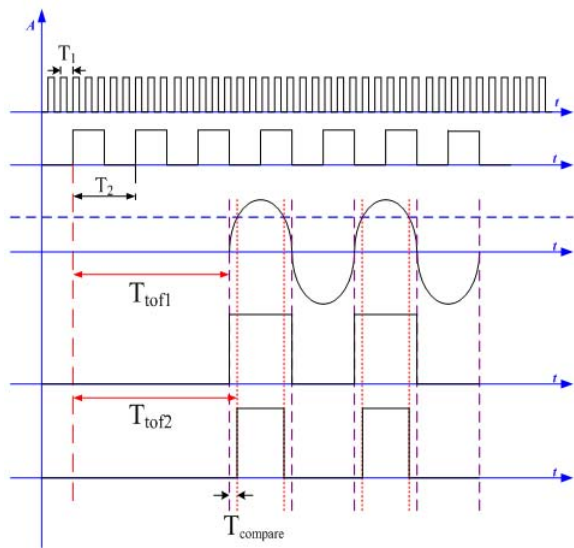


Fig. 9. Timing measurement schematic

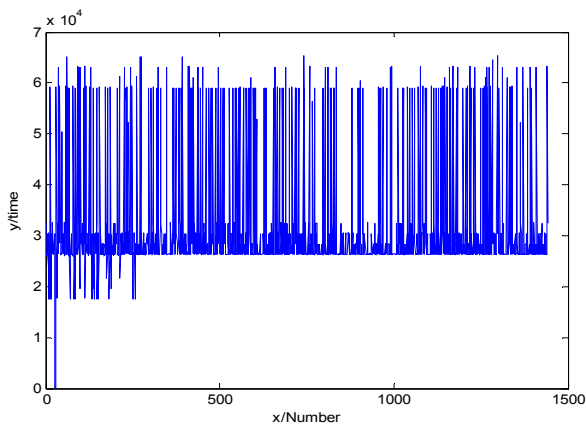


Fig. 10. Data Analysis

5. Experimental Results

The Records of flight time is shown in Figure 10. The Tcompare flag is very important in the system, we should select the Tcompare=0.2 v in experiment. The result will be stability. In case of no wind, the result is not zero using data analysis; there is interference with the environment.

6. Conclusions

Through the above analysis, the waveforms on the oscilloscope display well. In the experiment, we found the drive circuit for the sensor is extremely important especially when the sensitivity of ultrasonic sensor is not high because of ultrasound attenuation in the air. In the system the Tcompare's value is an important factor for the accuracy of system. Due to experimental condition, the system debugging has tested three points. In case of no wind $V_w = 0\text{m/s}$, we analyze the wind speed, the result is stable. When the wind speed is greater than 0m/s , the effect is unstable.

In experiment, we found that the signal amplification results displayed on the oscilloscope were unstable, the amplitude of the signal displayed on the oscilloscope becomes extremely unstable with the wind speed increased. When the wind speed is too large, the obtained data was very instable which effected the judge of the signal detection module. In the amplifier circuit, the amplified signal waveforms are stable after adding automatic gain amplifier module by setting the parameters. After verification, system stability has been further improved.

Acknowledgment

This paper is supported by United Lab of Technology and Applications for New Energy of the University of Electronic Science and Technology of China during the development of this project.

References

- [1] N.Roosnek. Novel digital signal processing techniques for ultrasonic gas flow measurements. Flow Instrumentation and Measurement, 2000,11(12):8999
- [2] N.Bignell. Ultrasonic Domestic Gas Meters-A Review. FLOMEK02000
- [3] J.G.de Carvalho, B.de C. Autunes. Measurement Using Ultra-sonic Transit-Time Method Some Aspects of Gas Flow Measurement. FLOMEK02000
- [4] H.Jeanneau, Geeuwke de Boer. Pipe Flow Modeling for Ultrasonic FlowMeasurement. FLOMEK02000
- [5] J.G.de Carvalho, B.de C.Autunes. Measurement Using Ultra-sonic Transit-Time Method Some spectrs of Gas Flow Measurement. FLOMEK02000
- [6] Miguel Perez del Valle, Jose Antonio Urbano Castelan., Low Cost Ultrasonic Anemometer, 2007 4th International Conference on Electrical and Electronics Engineering,Mexico, pp. 213-216, Sep. 2007.
- [7] SensComp, Inc.Piezo Transducers.July, 2003.
- [8] Ruo Feng, Ultrasound Technical Manual, Nanjing University Press, Nanjing, 1999.
- [9] MAXIM, Inc. http://china.maxim-ic.com/quick_view2.cfm/qv_pk/1452.
- [10] Altera Corporation, PLLs in Cyclone II Devices, Altera Corporation, 7-1, Feb, 2007.
- [11] Altera.Cyclone II Device Family Data Sheet. Altera Corporation, 2007.
- [12] Samir Palnitkar. Verilog HDL A Guide to Digital Design and Synthesis 2nd. Beijing: National Defence Industrial Press, 2004, 3-5